

# Wear behaviour of sintered steels obtained using powder metallurgy method

M. A. Erden\*, S. Gündüz\*\*, H. Karabulut\*\*\*, M. Türkmen\*\*\*\*

\*Karabuk University, 78050 Karabuk, Turkey, E-mail: makiferden@karabuk.edu.tr

\*\*Karabuk University, 78050 Karabuk, Turkey, E-mail: sgunduz@karabuk.edu.tr

\*\*\*Karabuk University, 78050 Karabuk, Turkey, E-mail: hasankarabulut@karabuk.edu.tr

\*\*\*\*Kocaeli University, Kocaeli, Turkey, E-mail: mustafa.turkmen@kocaeli.edu.tr,

crossref <http://dx.doi.org/10.5755/j01.mech.23.4.18982>

## 1. Introduction

Powder metal processing finds increasing application as they offer many advantages compared to other manufacturing processes. Greater alloying possibility and good self-lubricating capabilities permit economical manufacturing of complex shaped machine elements [1]. In addition to the typical advantages, PM steels present better microstructural features than conventional (wrought) steels such as homogeneity of carbide distribution in the matrix and smaller grain and carbide sizes, among others. Therefore some PM steels with high sintered density as well as high wear resistance have found wide application in the automotive industry, in engine and transmission systems, mainly for wear loaded components such as gears, sprockets and cam lobes [2, 3]. However, the wear behaviour research has been relatively scarce compared to steels manufactured by other routes [4-8].

In past years, mechanical properties of sintered steel were mainly studied by tensile and impact testing [9]. Today, demands for production of parts subjected to high mechanical loads and complex forces, e.g. engine parts and transmission gears need for the availability of dynamic properties such as wear and fatigue behaviour of sintered materials [10, 11]. Wear and fatigue are two of the major causes of engineering parts failure that start from surface or near the surface. The nucleation of crack occurs at the cluster of pores near the surface and propagates through the inter-pore ligaments. The lifetime decreases by increasing of total porosity [12].

Microalloyed steels are defined as steels containing small amounts of niobium, vanadium, or titanium, generally at levels between 0.05 and 0.20 wt.-%. Their specific

effects may be influenced by other alloying additions such as aluminium, boron, or indeed any of other more conventional alloying elements used in steel manufacture [13, 14]. The addition of microalloying elements offers an important cost-effective approach to obtain a good combination of excellent toughness and strength through grain size control and precipitation hardening. This is a result of the formation of carbonitrides, which lead to both precipitation strengthening and grain refinement [13, 15-17].

In this study dry sliding wear behaviour of the carbon steel Fe-0.25C (Alloy 1) and microalloyed steels Fe-0.25C-0.1Nb-Al (Alloy 2), Fe-0.25C-0.15Nb-Al (Alloy 3), Fe-0.25C-0.2Nb-Al (Alloy 4) was investigated. The effect of Nb and Al addition on hardness and wear properties of produced PM steels was discussed.

## 2. Experimental procedure

Fe, Nb and Al powders in the sizes of  $\leq 180$ ,  $< 45$ , and  $< 75$   $\mu\text{m}$  were used in the present study. The purity of Fe, Nb and Al was 99.9%, 99.8% and 93% respectively. The powders of Fe-0.25C (Alloy 1), Fe-0.25C-0.1Nb-Al (Alloy 2), Fe-0.25C-0.15Nb-Al (Alloy 3) and Fe-0.25C-0.2Nb-Al (Alloy 4) were mixed in an industrial conic mixer for 1 h and then cold pressed at 700 MPa with a die. The pressed PM steels were sintered at 1350 C for 1 h in the pure (99.999%) Ar gas atmosphere. Table 1 gives the chemical composition of the sintered PM steels. The size of the test specimens is 7 mm in length and 12 mm in diameter. The sintered density was measured by Archimedes' principle using pure water according to ASTM B 328-96 [18].

Table 1

Chemical composition of plain carbon PM steel and microalloyed PM steels (wt.-%)

	Fe	C	Al	Nb
Alloy 1	99.232	0.249	0.0000	0.0000
Alloy 2	98.5174	0.2355	0.0514	0.0468
Alloy 3	99.0191	0.2624	0.0752	0.0740
Alloy 4	99.0452	0.2653	0.0974	0.0918

Vickers hardness measurement was carried out in the 10 different areas of each specimen by using 1 kg load and average values were taken. The abrasive wear resistance of PM alloys was evaluated by using a standard pin-on-disc machine. The emery paper was fixed on a flat steel disc to serve as the abrasive medium. Test specimens for wear performance with length of 7 mm and diameter of

12 mm were rubbed on 320 mesh SiC paper at a sliding speed of 0.2 m/s. The applied loads were 10 N, 20 N, 30 N and the sliding distance was defined as 50 m. After wear tests, the specimens were cleaned carefully and weighed. The wear rate was calculated from the measured weight losses according to the Eq. (1) [19]:

$$w = \frac{\Delta m \times 1000}{ql} \quad (1)$$

where  $w$  is the wear rate,  $\text{mm}^3 \text{m}^{-1}$ ;  $\Delta m$  is the weight loss, g;  $q$  is the density,  $\text{g cm}^{-3}$  and  $l$  is the sliding distance on the grinding paper, m.

Steel microstructure and worn surfaces of the specimens were examined by using optical microscope and scanning electron microscope (SEM). Samples for metallographic examination were prepared by grinding, polishing and etching techniques to reveal the grains and phases. A Nikon ECLIPSE L150 type microscope capable to magnify from  $50\times$  to  $1000\times$  was used for optical examination. The grain sizes were measured by using mean linear intercept (mli) method on etched metallographic specimens. The volume fraction of ferrite or pearlite was also measured by using the point count method. Worn surfaces of the specimens representing the various testing conditions were analysed with scanning electron microscopy (JEOL 5600 JSM). In addition to the microstructure examination, the surface roughness coefficient  $R_a$ , showing the mean arithmetic surface profile deviation, was also measured with the Mitutoya Surftest 211 profilometer on all PM steel specimens. Three measurements were made on each surface.

### 3. Results and discussion

#### 3.1. Microstructure and hardness

Fig. 1 shows the structure of the plain carbon PM steel and microalloyed PM steels. As can be seen, steels consisted of ferrite and pearlite structure with varying grain sizes. A number of tiny pores could also be seen in the Fig. 1. Microstructure characteristics of the sintered plain carbon PM steel and microalloyed PM steels are given in Table 2, which showed grain sizes decreased when

the Nb-Al content increased to 0.1, 0.15 or 0.2 wt.-%. These changes would be expected as a result of the differences in precipitation distribution [20]. The microalloying elements prevent the motion of grain boundaries, recrystallisation boundaries and dislocations when they are present either as solute atoms or precipitate particles. Therefore, the microalloying elements can suppress grain coarsening, static recrystallization and the motion of dislocations. When they are in solid solution in austenite, these elements can also lead to lower transformation temperatures [21]. If fine precipitates exist during the austenitizing step, the motion of crystal defects is restricted, leading to a finer grain size after quenching [14, 22].

The density also significantly affects the properties of plain carbon PM steel and microalloyed PM steels. Sintering density of PM steels depends on pressing load, particle size, added alloying elements and sintering temperature and time. It is known that density and microstructure in PM steels are the most important factors determining the mechanical properties [23]. Mechanical properties of PM steels can also be effected by the presence of precipitate particles such as NbC(N) and AlN. As seen from Fig. 2 that hardness increased as the Nb-Al content increased to 0.1, 0.15 or 0.2 wt.-%.

The microalloying elements produce precipitation of carbonitrides in austenite, and the pro-eutectoid ferrite and pearlite phases of the final microstructure in order to obtain grain refinement and precipitation strengthening [24]. The behaviour of microalloying elements can be modified by the presence of another of them and changes dependent on a particular elements. In principle it depends on their solid insolubility or solid solubility. AlN has a close packed hexagonal structure, with little or no solubility for niobium and NbN has a cubic structure with little or no solubility for aluminium. At these conditions, the two separate nitrides can co-exist in the austenite according to their own solubility products [25]. During sintering and

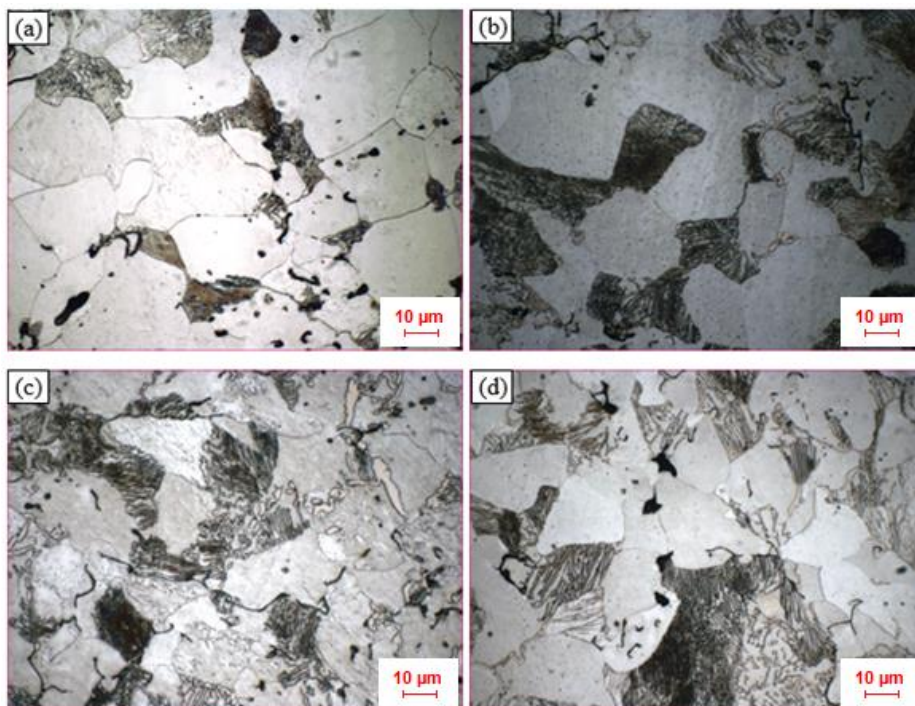


Fig. 1 Microstructures of sintered plain carbon PM steel and microalloyed PM steels: a - Alloy 1; b - Alloy 2; c - Alloy 3; d - Alloy 4

Properties of the investigated as-sintered plain carbon PM steel and microalloyed PM steels

Alloy	Sintered Density, $\text{g cm}^3$	Grain Size, $\mu\text{m}$	Ferrite, %	Pearlite, %
Alloy 1	7.208	29	78	22
Alloy 2	7.358	27	75	25
Alloy 3	7.357	23	74	26
Alloy 4	7.356	22	73	27

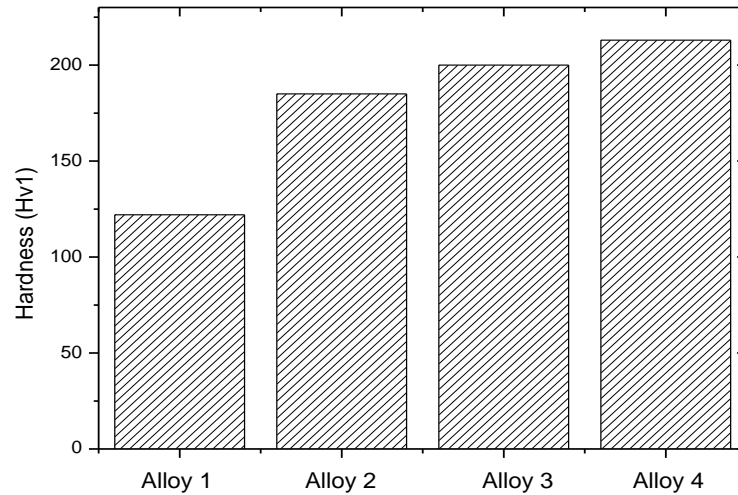


Fig. 2 Hardness results of plain carbon PM steel (Alloy 1) and microalloyed PM steels (Alloys 2-4)

slow cooling from sintering temperature the microalloying elements Nb and Al form a precipitate in the matrix such as NbC(N) or AlN. These precipitates formed when there are sufficient amounts of Nb and Al present in the form of a solid solution in austenite during the transformation stage at the upper critical temperature as suggested by Erden et al [26]. Hence, hardness of the microalloyed PM steels showed higher values compared with the plain carbon PM steel.

In the present experimental work plain carbon PM steel and microalloyed PM steels showed similar sintered density of  $7.20 \text{ g cm}^{-3}$  and  $7.35 \text{ g cm}^{-3}$  respectively. It can be explained that hardness increment in microalloyed PM steels is due to the precipitation of NbC(N), AlN and finer

ferrite and pearlite structure. The precipitation of NbC(N) and AlN particles during sintering or cooling after sintering increases the hardness of microalloyed PM steels. These results are consistent with the results obtained from earlier studies [27, 28]. Fig. 3 shows example of a particle found in Alloy 4 (Fe-0.25C-0.2Nb-Al) with its corresponding EDS analysis. As seen from Fig. 3 that this EDS analysis confirms the presence of Fe, C, N, Al, Nb elements in precipitate particle. Concerning the literature and the current results, the presence of these elements indicates NbC(N) and AlN particles occurred during sintering and/or cooling after sintering. The results of EDS analysis agree with the precipitates visible on the SEM micrograph of microalloyed PM steels.

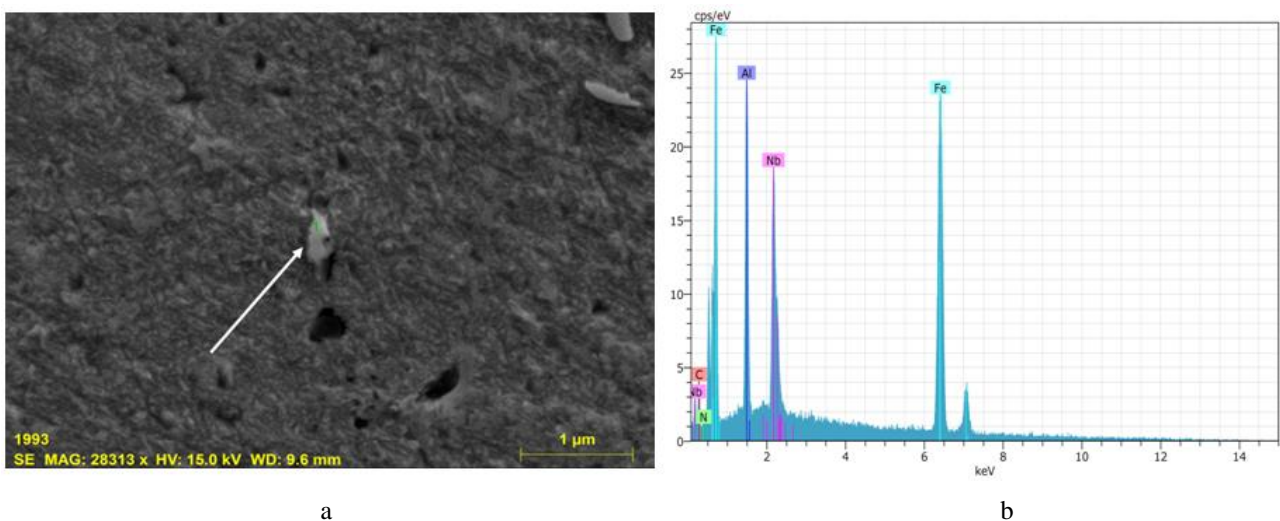


Fig. 3 a - SEM micrograph for Alloy 4 and b - corresponding EDS of the indicated precipitate particle

### 3.2. Wear behaviour of PM alloys

Fig. 4 illustrates the effect of Nb-Al content and wear loads on wear resistance of the plain carbon PM steel and microalloyed PM steels. It can be seen that wear rate decreased when the Nb-Al content was increased to 0.1, 0.15 or 0.2 wt.-%. This shows that the wear behaviour of the steels depended on the hardness and microstructural alterations occurred during sintering at 1350°C or cooling after sintering. The highest and lowest wear rate were obtained in the Alloy 1 and Alloy 4 at the sliding distance of 50 m and the wear loads of 10 N, 20 N and 30 N. Higher wear rate were observed in Alloy 1 due to lower hardness. In their work Sudhakar et al. [29] investigated wear behaviour of Fe-2%Ni based PM steel and showed that the wear

rate increased with a decrease in hardness level.

Alloy 4 exhibited the lowest wear rate due to increased hardness as a result of the precipitation of NbC(N) and AlN providing strengthening and fine grain sizes in steel. These results are comparable with Gündüz et al. [30] who showed that vanadium addition in the percentage of 0.08% raised hardness and wear resistance by precipitation strengthening and by refining the pearlite. Strafelini and Molinari [31] also showed that an increase in density and hardness caused an improvement of wear resistance of PM steels. It is clear from the foregoing discussion that hardness and wear are closely related, so that high hardness leads to reduced wear rate. The precipitation of NbC(N) and AlN particles and low grain size results in high hardness [32, 33], which in turn reduces wear.

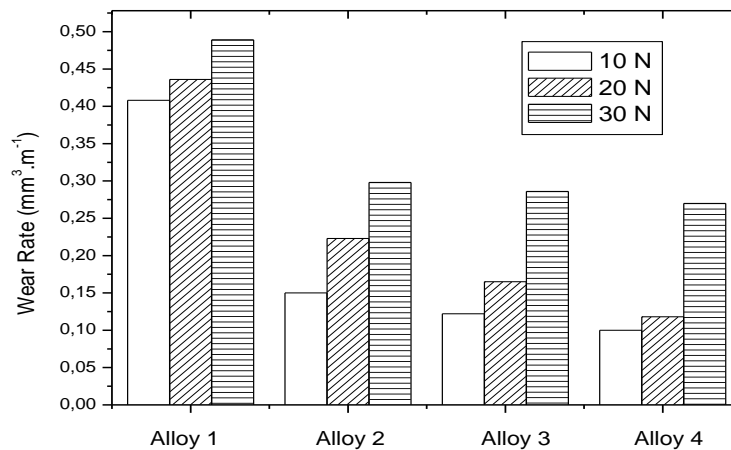


Fig. 4 Wear rate of plain carbon PM steel (Alloy 1) and microalloyed PM steels (Alloys 2-4)

Wear rates as a function of the loads is given in Fig. 4. As seen, wear rates of all PM steels tested at a load of 10 N are lower than that of the all PM steels tested at the loads of 20 N or 30 N. The wear rate drastically increased when the loads increased to 20 N or 30 N. This is consistent with the general principle of wear [34]. As also seen from Fig. 4 that wear rate showed lowest values at the minimum load of 10 N irrespective of the alloy composition. Tribological behavior of metals which are in sliding contact depends on the many variables such as normal load applied on the material, sliding speed, sliding distance, surface geometry, surface hardness, roughness of operating surface, working environment, etc., which affect the wear mechanism and results in change of wear rate [35]. Tripathy [36] behaviour of modified 9Cr-1Mo steel. The results obtained for the annealed samples exposed to three different load variations of 30 N, 50 N and 100 N shows that with increase in load, the wear rate increases as there is increase in friction at the contact surface. The results obtained from the present work indicated that wear loads should be carefully chosen in order to avoid high component wear.

Fig. 5 shows the worn surfaces of plain carbon PM steel and microalloyed PM steels tested at 20 N. The scratches seen on the worn surfaces reveals the rate of wear occurs and also the direction in which the wear occurs and pattern it follows. Worn surface pattern revealed that the wear mechanism is ploughing. The surface exhibited extensive grooving occurred as a result of ploughing by the harder SiC paper. All produced PM steels exhibited plastic grooves parallel to sliding direction. For example, a

great deal of wear grooves was formed along the sliding direction as indicated by the vertical arrow on the surface of Alloy 1 and Alloy 2 (Figs. 5, a and 5, b). On the worn surface of the Alloy 3 and Alloy 4 (Figs. 5, c and 5, d), however, the damaged regions disappear and the grooves become much narrower and shallower. This is evident that the worn surface damage decreased when the hardness of microalloyed PM steels increased.

Mechanical properties affecting wear resistance of a material include hardness, fracture toughness, elastic modulus, tensile/compressive strength, and impact fatigue strength. In many cases, wear resistance is primarily a function of hardness not of toughness, especially for metal alloys which have sufficient fracture toughness. The higher the hardness, the higher the resistance to abrasion by hard particles, surface plastic deformation, debonding, and microploughing [37]. Wear behavior can also greatly be affected by crystal structure, grain size, and grain boundaries. The presence of grain boundaries in polycrystalline materials influences friction as well as wear behaviour. When sliding motion occurs, surface dislocations are blocked in their movement by a grain boundary and they accumulate at the grain boundary which results in strain-hardening of the surface layers. This action makes sliding motion more difficult and increases frictional force for materials in sliding contact leads to wear of the material [38]. Fig. 5, e shows the EDS pattern of Alloy 4 tested at 20N. This pattern reveals the presence of aluminium and oxygen elements which is marked as AIO on the wear surface of Alloy.

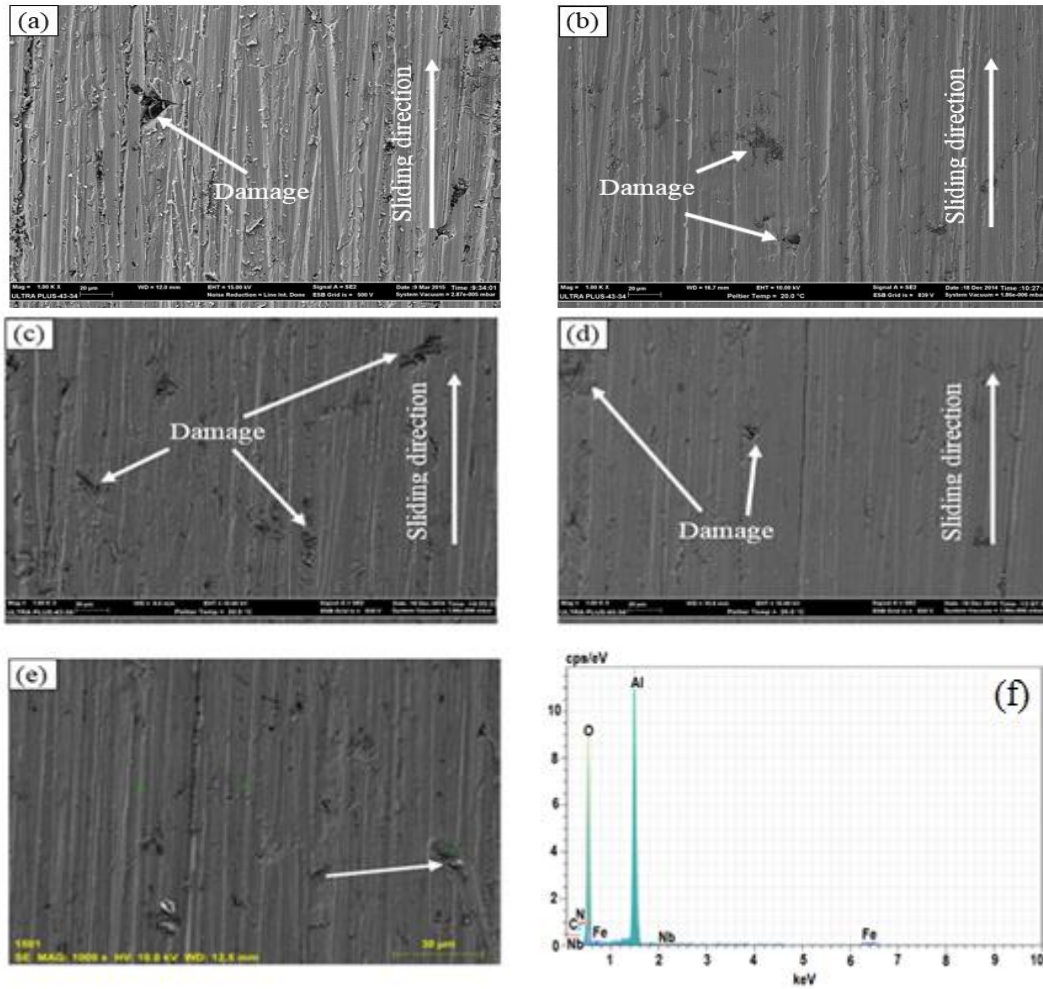


Fig. 5 SEM wear images of sintered plain carbon PM steel and microalloyed PM steels tested at 20N: a - Alloy 1; b - Alloy 2; c - Alloy 3; d - Alloy 4; e and f - EDS results from indicated particle of Alloy

In most industrial applications, the surface quality is of a great importance [39]. In this work, the surface roughness of plain carbon PM steel and microalloyed PM steels tested at 30 N was measured. The surface roughness coefficient  $R_a$ , showing the average arithmetic profile deviation, was determined. Fig. 6 reveals the results of  $R_a$  measurements. These values are the averages of three readings. It can be seen that continuous decrease in surface roughness was observed when the Al-Nb content increased to 0.1, 0.15 or 0.2 wt.-%. This is due to their different

hardness values obtained after sintering. For example, Alloy 4 had the lowest surface roughness values compared to Alloys 1-3. That is because, hardness of Alloy 4 is the highest. These alloys with different hardness values will result in different wear behaviour. Şeker at al. [40] showed that the surface roughness values obtained for the alloyed ductile specimens are better than that of the unalloyed specimen by at least approximately 50%. This was explained by their higher hardness.

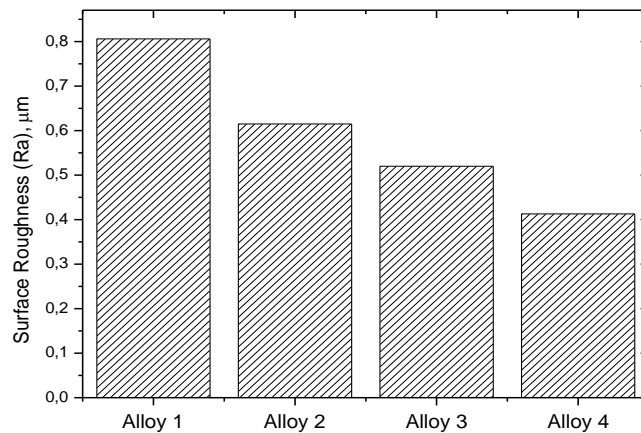


Fig. 6 Surface roughness of worn steel specimens for plain carbon PM steel (Alloy 1) and microalloyed PM steels (Alloys 2-4)

## 5. Conclusion

In the present study, the abrasive wear behaviour of plain carbon PM steel and microalloyed PM steels has been evaluated by a pin-on-disc machine. Based on the results obtained the following important conclusions could be drawn from the wear experiments on the PM steels:

1. Nb-Al microalloying addition to Fe-0.25%C alloy steel system is found to enhance the hardness and wear resistance. The wear rate decreases with increasing hardness of the sintered PM steels investigated.

2. Plain carbon steel (Fe-0.25%C) is subjected to higher wear rate and due to the presence of ferrite and pearlite in the microstructure.

3. All alloys exhibited plastic grooves parallel to sliding direction, however, the damaged regions disappear and the grooves become much narrower and shallower when the hardness of microalloyed PM steels increased.

4. Continuous decrease in surface roughness of microalloyed PM steels was observed with an increase in alloying elements. This is due to their different hardness values obtained after sintering.

## Acknowledgements

The authors gratefully acknowledge financial support from (TÜBİTAK) the Research Project of The Scientific and Technological Research Council of Turkey with the NO: 113M350.

## References

- Dhanasekaran, S.; Gnanamoorthy, R.** 2007. Abrasive wear behavior of sintered steels prepared with MoS<sub>2</sub> addition, *Wear* 262(5-6): 617-623. <http://dx.doi.org/10.1016/j.wear.2006.07.006>.
- Hortenhuber, A.** 1992. PM camshaft technology, *Metal Powder Rep.* 47(1): 16-19. [http://dx.doi.org/10.1016/0026-0657\(92\)91823-3](http://dx.doi.org/10.1016/0026-0657(92)91823-3).
- Babakhani, A.; Haerian, A.; Ghambri, M.** 2008. Effect of heat treatment, lubricant and sintering temperature on dry sliding wear behavior of medium alloyed chromium PM steels, *Journal of Materials Processing Technology* 204(1-3): 192-198. <http://dx.doi.org/10.1016/j.jmatprotec.2007.11.061>.
- Vardavoulias, M.; Jouanny-Tresy, C.; Jeandin, M.** 1993. Sliding-wear behaviour of ceramic particle-reinforced high-speed steel obtained by powder metallurgy, *Wear* 165(2): 141-149. [http://dx.doi.org/10.1016/0043-1648\(93\)90329-K](http://dx.doi.org/10.1016/0043-1648(93)90329-K).
- El-Rakayby, A.M.; Mills, B.** 1986. Tempering and secondary hardening of M 42 high-speed steel, *Materials Science and Technology* 2(2): 175-180. <http://dx.doi.org/10.1179/mst.1986.2.2.175>.
- Vardavoulias, M.; Jeandin, M.; Grillon, F.** 1993. Effects of tempering on the sliding wear behaviour of A sintered high-speed steel – A quantitative image analysis approach, *Scripta Metallurgica et Materialia* 29(3): 359-364. [http://dx.doi.org/10.1016/0956-716X\(93\)90513-R](http://dx.doi.org/10.1016/0956-716X(93)90513-R).
- Vardavoulias, M.** 1994. The role of hard second phases in the mild oxidational wear mechanism of high-speed steel-based materials, *Wear* (1-2), 173: 105-114. [http://dx.doi.org/10.1016/0043-1648\(94\)90262-3](http://dx.doi.org/10.1016/0043-1648(94)90262-3).
- Wang, J.; Danninger, H.** 1998. Dry sliding wear behavior of molybdenum alloyed sintered steels, *Wear* 222(1): 49-56. [http://dx.doi.org/10.1016/S0043-1648\(98\)00279-8](http://dx.doi.org/10.1016/S0043-1648(98)00279-8).
- Hausner, H.H.; Mal, K.** 1982. *Handbook of Powder Metallurgy*, New York: Chemical Publications.
- Danninger, H.; Spoljaric, D.; Weiss, B.** 1997. Microstructural features limiting the performance of PM steels, *International Journal of Powder Metallurgy* 33(4): 43-53.
- Lim, S.C.; Lim, C.Y.H.; Lee, K.S.** 2002. The effects of machining conditions on the flank wear of TiN-coated high speed steel tool inserts, *Wear* 181-183(2): 901-912.
- Khorsand, H.; Habibi, S.M.; Yoozbashizadea, H.; Janghorban, K.; Reihani, S.M.S.; Rahmani Seraji, H.; Ashtari, M.** 2002. The role of heat treatment on wear behavior of powder metallurgy low alloy steels, *Materials and Design* 23(7): 667-670. [http://dx.doi.org/10.1016/S0261-3069\(02\)00046-8](http://dx.doi.org/10.1016/S0261-3069(02)00046-8).
- Schade, C.; Murphy, T.; Lawley, A.; Doherty, R.** 2012. Microstructure and mechanical properties of microalloyed PM steels, *International Journal of Powder Metallurgy* 48(3): 51-59.
- Gladman, T.** 1997. *The Physical Metallurgy of Microalloyed Steels*, 1st ed., The institute of Materials, London, 363 p.
- Bakkali El Hassania, F.; Chenaouia, A.; Dkiouak, R.; Elbakkali, L.; Al Omar, A.** 2008. Characterization of deformation stability of medium carbon microalloyed steel during hot forging using phenomenological and continuum criteria, *Journal of Materials Processing Technology* 199(1-3): 140-149. <http://dx.doi.org/10.1016/j.jmatprotec.2007.08.004>.
- Show, B.K.; Veerababu, R.; Balamuralikrishnan, R.; Malakondaiah, G.** 2010. Effect of vanadium and titanium modification on the microstructure and mechanical properties of a microalloyed HSLA steel, *Materials Science and Engineering: A*, 527(6): 1595-1604. <http://dx.doi.org/10.1016/j.msea.2009.10.049>.
- Zhao, J.; Lee, J.H.; Kim, Y.W.; Jiang, Z.; Lee, C.S.** 2013. Enhancing mechanical properties of a low-carbon microalloyed cast steel by controlled heat treatment, *Materials Science and Engineering: A*, 559(1): 427-435. <http://dx.doi.org/10.1016/j.msea.2012.08.122>.
- Standard Test Method for Density, Oil Content, and Interconnected Porosity of Sintered Metal Structural Parts and Oil-Impregnated Bearings, ASTM B328-96, ASTM International (Philadelphia, USA, 2004).
- Czicos, H.** 1978. *Tribology: a System Approach to the Science and Technology of Friction, Lubrication and wear*, Elsevier Scientific Publishing Company, Amsterdam, 400 p.
- Karabulut, H.; Gündüz, S.** 2004. Effect of vanadium content on dynamic strain ageing in microalloyed medium carbon steel, *Materials Design* 25(6): 521-527. <http://dx.doi.org/10.1016/j.matdes.2004.01.005>.
- DeArdo, A.J.; Garcia, C.I.; Palmiere, E.J.** 1991. *Thermomechanical Processing of Steels*, 10th ed., Metals Handbook.
- Schade, C.; Murphy, T.; Lawley, A.; Doherty, R.** 2012. Microstructure and mechanical properties of PM steels alloyed with silicon and vanadium, *International*

- Journal of Powder Metallurgy 48(6): 41-48.
23. **Tekeli, S.; Güral, A.; Özyürek, D.** 2007. Dry sliding wear behaviour of low carbon dual phase powder metallurgy steels, *Materials and Design* 28(5): 1685-1688. <http://dx.doi.org/10.1016/j.matdes.2006.03.013>.
  24. **Parsons, S.A.; Edmonds, D.V.** 1987. Microstructure and mechanical properties of medium-carbon ferrite-pearlite steels microalloyed with vanadium, *Materials Science Technology* 3: 894-904. <http://dx.doi.org/10.1179/mst.1987.3.11.894>.
  25. **Gladman, T.; in: Tither, G.; Shouhua, Z. eds.** 2014. *The Minerals, Metals and Materials Society* 3: 267-271.
  26. **Erden, M.A.; Gündüz, S.; Türkmen, M.; Karabulut, H.** 2014. Microstructural characterization and mechanical properties of microalloyed powder metallurgy steels, *Materials Science and Engineering: A*, 616: 201-206. <http://dx.doi.org/10.1016/j.msea.2014.08.026>.
  27. **Ghosh, A.; Das, S.; Chatterjee, S.; Mishra, B.; Ramachandra Rao, P.** 2006. Effect of cooling rate on structure and properties of an ultra-low carbon HSLA-100 grade steel, *Material Characterization* 56: 59-65. <http://dx.doi.org/10.1016/j.matchar.2005.09.014>.
  28. **Kaynar, A.; Gündüz, S.; Türkmen, M.** 2013. Investigation on the behaviour of medium carbon and vanadium microalloyed steels by hot forging test, *Materials and Design* 51: 819-825. <http://dx.doi.org/10.1016/J.MATDES.2013.04.102>.
  29. **Sudhakar, K.V.; Sampathkumaran, P.; Dwarakadasa, E.S.** 2000. Dry sliding wear in high density Fe-2%Ni based P r M alloys, *Wear* 242(1-2): 207-212. [http://dx.doi.org/10.1016/S0043-1648\(00\)00422-1](http://dx.doi.org/10.1016/S0043-1648(00)00422-1).
  30. **Gündüz, S.; Kaçar, R.; Soykan, H.S.** 2008. Wear behaviour of forging steels with different microstructure during dry sliding, *Tribology International* 41(5): 348-355. <http://dx.doi.org/10.1016/j.triboint.2007.09.002>.
  31. **Straffelini, G.; Molinari, A.** 2001. Dry sliding wear of ferrous PM materials, *Powder Metallurgy* 44(3): 248-252. <http://dx.doi.org/10.1179/003258901666419>.
  32. **Dieter, G.E.** 1976. *Mechanical Metallurgy*, 3rd ed. McGraw-Hill, 800 p.
  33. **Rahimian, M.; Parvin, N.; Ehsani, N.** 2011. The effect of production parameters on microstructure and wear resistance of powder metallurgy Al-Al<sub>2</sub>O<sub>3</sub> composite, *Materials and Design* 32: 1031-1038. <http://dx.doi.org/10.1016/j.matdes.2010.07.016>.
  34. **Kandavel, T.K.; Chandramouli, R.; Manoj, M.; Manoj, B.; Kumar Gupta, D.** 2013. Influence of copper and molybdenum on dry sliding wear behaviour of sintered plain carbon steel, *Materials and Design* 50: 728-736. <http://dx.doi.org/10.1016/j.matdes.2013.03.037>.
  35. **Devaraju, A.; Elayaperumal, A.** 2010. Tribological behaviours of plasma nitrided AISI 316 LN type stainless steel in air and high vacuum atmosphere at room temperature, *International Journal of Engineering Science and Technology* 2: 4137-4146.
  36. **Tripathy, İ.** 2011. Effect of microstructure on sliding wear behaviour of modified 9Cr-1Mo steel, MSc Thesis, Rourkela, India.
  37. **Zhigang Fang; Smith Tool; Smith International** Wear resistance of powder metallurgy alloys, ASM Handbook Volume 7, Powder Metal Technologies and Applications (ASM International).
  38. **Bhushan, B.; Gupta, B.K.** 1990. *Handbook of Tribology, Materials, Coatings and Surface Treatments*, McGraw-Hill.
  39. **Novak, P.; Vojtech, D.; Serak, J.** 2006. Wear and corrosion resistance of a plasma-nitrided PM tool steel alloyed with niobium, *Surface & Coatings Technology* 200: 5229-5236. <http://dx.doi.org/10.1016/j.surfcoat.2005.06.023>.
  40. **Şeker, U.; Çiftçi, İ.; Hasırcı, H.** 2003. The effect of alloying elements on surface roughness and cutting forces during machining of ductile iron, *Materials and Design* 24: 47-51. [http://dx.doi.org/10.1016/S0261-3069\(02\)00081-X](http://dx.doi.org/10.1016/S0261-3069(02)00081-X).

M. A. Erden, S. Gündüz, H. Karabulut, M. Türkmen

#### WEAR BEHAVIOUR OF SINTERED STEELS OBTAINED USING POWDER METALLURGY METHOD

#### S u m m a r y

In this work, the hardness and abrasive-wear behaviour of powder metallurgy (PM) plain carbon steel and microalloyed steels with different amount of niobium or aluminium content (0.1-02 wt.-%) were investigated. It was found that steels microalloyed by niobium and aluminium have high hardness and wear resistance compared with the niobium and aluminium free steel. Wear behavior of these steels depends on the PM processing parameters and wear conditions. Worn surface pattern revealed the wear mechanism is ploughing. The surface exhibited extensive grooving occurred as a result of ploughing by the harder SiC paper.

**Keywords:** Steel; Sliding wear; Hardness; Surface topography.

Received March 31, 2016

Accepted August 04, 2017